Pergamon

Tetrahedron 58 (2002) 661–671

TETRAHEDRON

Cation-directed self-assembly of lipophilic nucleosides: the cation's central role in the structure and dynamics of a hydrogen-bonded assembly

Mangmang Cai,[a] Xiaodong Shi,[a] Vladimir Sidorov,[a] Daniele Fabris,[b] Yiu-fai Lam[a] and Jeffery T. Davis[a,*]

[a]*Department of Chemistry and Biochemistry, University of Maryland at College Park, College Park, MD 20742, USA*
[b]*Department of Chemistry and Biochemistry, University of Maryland, Baltimore County, Baltimore, MD 21228, USA*

Received 6 June 2001; revised 27 August 2001; accepted 28 August 2001

Abstract—This paper focuses on the cation's central role in controlling the self-assembly of a lipophilic nucleoside, isoguanosine (isoG) **2**, in organic solvents. First, we use ^{1}H NMR spectroscopy to show that a Ba^{2+} cation directs a mixture of the isomers isoG **2** and guanosine (G) **1** to self-sort into separate assemblies, without any detectable G–isoG cross-association. Next, we use electrospray ionization mass spectrometry to show that the cation controls the reversible self-assembly of isoG **2**. Final section focuses on the dynamic exchange of components between two different assemblies, namely, a (isoG **2**)$_5$–Li^+ pentamer and a (isoG **2**)$_{10}$–Li^+ decamer. Our ^{1}H and ^{7}Li NMR data is consistent with a cation-filled pentamer, (isoG **2**)$_5$–Li^+, moving as a unit during a bimolecular pentamer–decamer exchange. These data highlight crucial aspects regarding the cation-templated self-assembly of lipophilic nucleosides: (1) the structural information encoded within each nucleoside dictates the size and shape of the hydrogen-bonded assembly; (2) a cation is required to template and stabilize these discrete hydrogen-bonded assemblies, and (3) dynamic exchange of cation-filled, hydrogen-bonded units is likely to be a hallmark of these multi-layered nucleoside assemblies.

1. Introduction

Self-assembly involves organization of molecules into discrete aggregates held together by non-covalent interactions.[1] Many different building blocks have been designed to give self-assembled systems with various forms and functions.[1–4] Usually, hydrogen bonds[2] or coordination bonds[3,4] drive the self-assembly. Instead of a de novo approach, we have been using modified natural products, such as guanosine (G) **1** and isoguanosine (isoG) **2** to form non-covalent assemblies that have both hydrogen bonds and cation–dipole interactions. In the presence of alkali or alkaline earth cations, these lipophilic nucleosides form discrete hydrogen-bonded aggregates in organic solvents.[5–8] We envision that assemblies formed from G **1**, isoG **2**, and analogs, may be useful for ion separations,[9] catalysis,[10] and as artificial ion channels.[11]

In the molecular recognition field, various nucleobase derivatives have been used to construct interesting and functional noncovalent structures.[12] These systems usually rely on Watson–Crick or Hoogsteen base pairing. Indeed, our original intent was to determine if G **1** and isoG **2** would form a Watson–Crick base pair (Scheme 1).[13] In the process, we found that G **1** and isoG **2** self-associate in a cation-dependent process to give hydrogen-bonded macrocycles in organic solvents. Crystal structures show that G **1** forms assemblies based on hydrogen-bonded tetramers (G-quartets),[14,15] and isoG **2** gives hydrogen-bonded pentamers.[16] The G-quartet is a well-known motif in nucleotide and DNA structure,[17,18] while a pentaplex has been

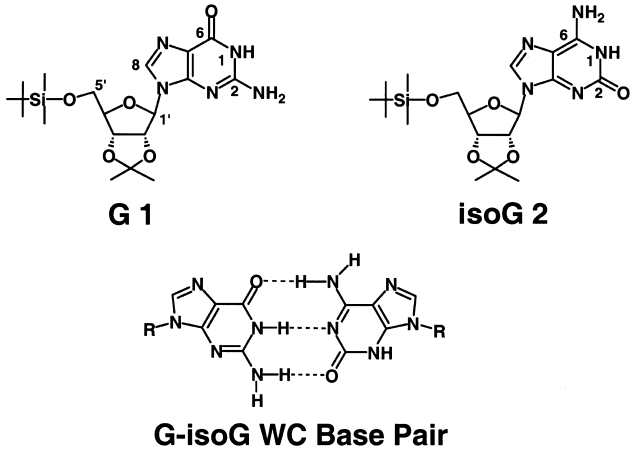

Scheme 1.

Keywords: lipophilic nucleoside; hydrogen-bonded assembly; self-assembly.

* Corresponding author. Tel.: +1-304-405-1845; fax: +1-301-314-9121; e-mail: jd14@umail.umd.edu

0040–4020/02/$ - see front matter
PII: S0040-4020(01)01101-2

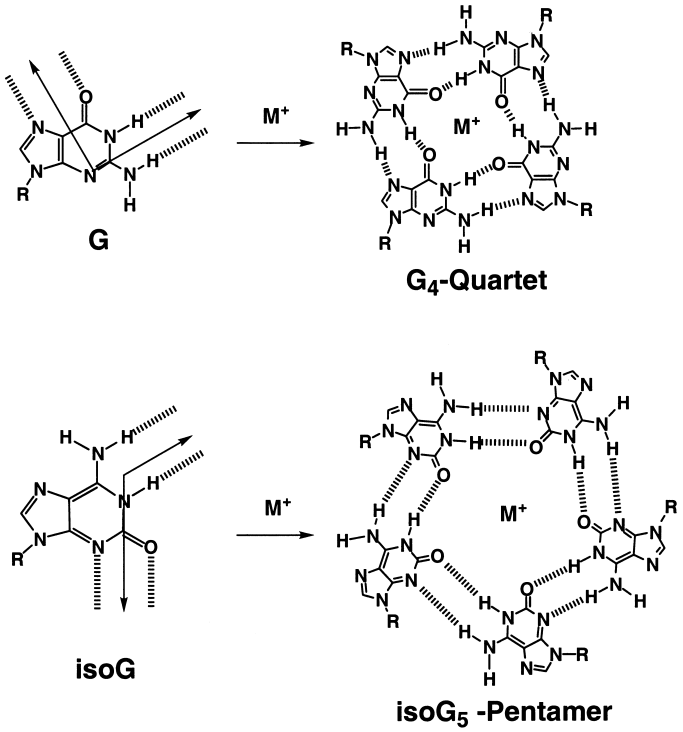

Scheme 2. Both G and isoG self-associate in the presence of cations to give either hydrogen-bonded G_4-quartets or $isoG_5$-pentamers. The relative orientation of the nucleoside's hydrogen bond donor and acceptor groups determines the assembly's size.

formed from isoG-oligonucleotides and Cs^+.[19] These different self-assembled units can be ascribed to the orientation of the nucleobase's hydrogen bonding groups (Scheme 2).[16,19] Guanosine has a 90° angle between its guanidinium donor and Hoogsteen acceptor face, a perfect orientation for a planar quartet. The angle between isoG's hydrogen bonding donor and acceptor groups is close to 110°, favoring a cyclic pentamer. In these systems, a cation is almost always required to stabilize the hydrogen-bonded macrocycles.[20]

With regard to the alkali ions, the G-quartet from G **1** is moderately selective for binding K^+ over Na^+ and Rb^+. In contrast, the expanded isoG pentamer is highly selective for binding the larger Cs^+ ion,[9,16] although isoG **2** will complex all of the alkali cations.[5] Both G **1** and isoG **2** can further aggregate by cation-stabilized stacking of hydrogen-bonded layers. Thus, G **1** forms a hexadecamer composed of four stacked G-quartets,[14,15] while isoG **2** gives a sandwich decamer $[\text{isoG } \mathbf{2}]_{10}\cdot M^+$ (Scheme 3).[5,16] While isoG **2** and G **1** differ only in the transposition of an oxygen and nitrogen atom, this simple change in molecular structure leads to significant differences in the supramolecular organization and cation selectivity for the two assemblies.

2. Paper's organization

This paper focuses on the cation's central role in controlling the self-assembly of isoG **2**. First, we use ^{1}H NMR spectroscopy to show that a cation can direct a mixture of isoG **2** and G **1** to self-sort into separate assemblies, without detectable G–isoG cross-association. Next, we use mass spectrometry to show that the cation controls the reversible self-assembly of isoG **2**. The paper's final section focuses on the dynamic exchange of components between two different assemblies, a $(\text{isoG } \mathbf{2})_5\cdot Li^+$ pentamer and a $(\text{isoG } \mathbf{2})_{10}\cdot Li^+$ decamer. Our ^{1}H and ^{7}Li NMR data are consistent with a

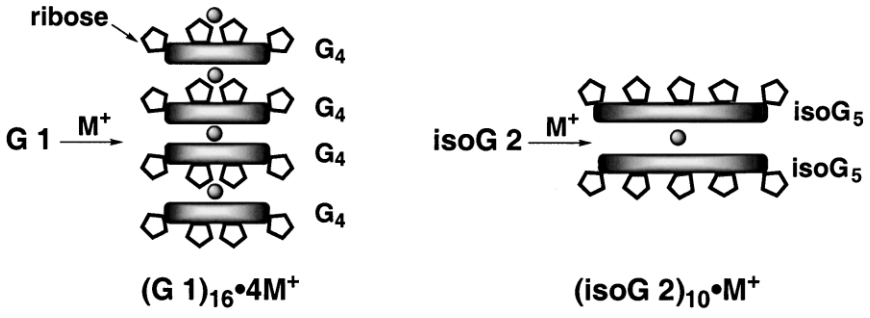

Scheme 3. The G_4-quartets and $isoG_5$-pentamers stack in the presence of cations. G **1** binds metal cations to give a hexadecamer composed of four G_4-quartets. IsoG **2** binds metal cations to form a sandwich decamer.

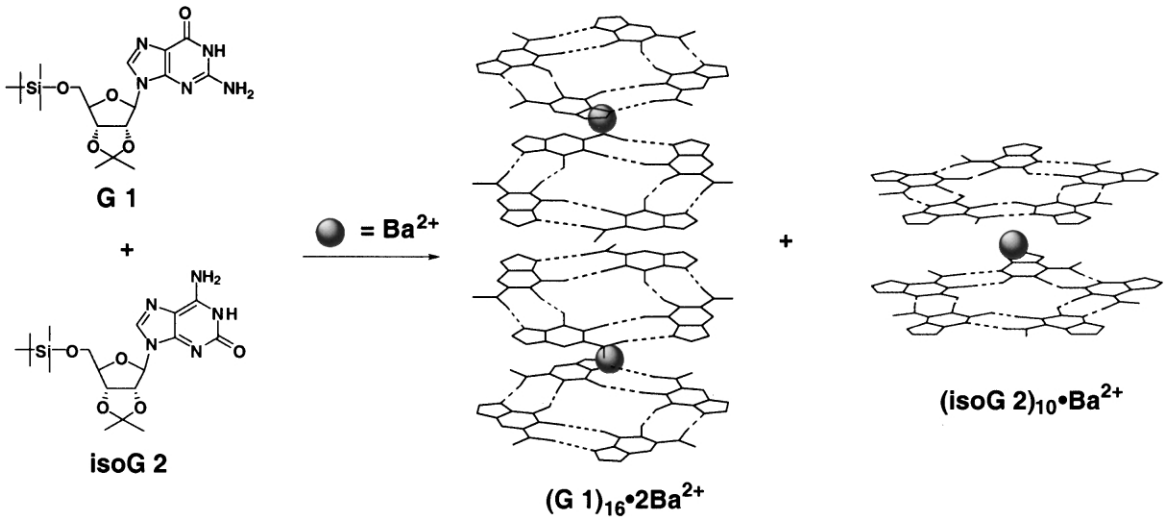

Scheme 4. The isomers G **1** and isoG **2** 'self-sort' in the presence of barium picrate to give discrete complexes.

cation-filled pentamer, (isoG **2**)$_5$·Li$^+$, moving as a unit during a bimolecular pentamer–decamer exchange reaction. These data highlight crucial aspects regarding self-assembly of these lipophilic nucleosides: (1) the structural information encoded within each nucleoside dictates the size and shape of the hydrogen-bonded assembly; (2) the cation is required to template and stabilize these discrete hydrogen-bonded assemblies, and (3) dynamic exchange of cation-filled, hydrogen-bonded units is likely to be a hallmark of these multi-layered nucleoside assemblies.

3. Cation-templated self-sorting of G 1 and isoG 2

Both G **1** and isoG **2** self-associate to give hydrogen-bonded macrocycles, provided a cation is available.[15,16] What happens when isoG **2** and G **1** are together in solution, with cations in the mix? These isomers could form various G–isoG base pairs,[13] or they could self-sort[21] to give segregated complexes (Scheme 4). Below, we show that Ba^{2+} directs efficient formation of G-quartet and isoG pentamer structures from a mixture of the two nucleosides.[22]

A comparison of Fig. 1A–C indicates that the isomers G **1** and isoG **2** do *cross-associate* when mixed together in CD_2Cl_2 in the absence of cations. Fig. 1C shows that G **1** and isoG **2** give a relatively complicated ^{1}H NMR spectrum when combined in CD_2Cl_2. This ill-defined spectrum is likely due to the formation of different hydrogen-bonded aggregates of similar free energies. In contrast, the addition of Ba^{2+} to a mixture of G **1** and isoG **2** results in a well-defined NMR spectrum consistent with formation of discrete hydrogen-bonded complexes (Fig. 1F).

Before doing the *mixing* experiment with the isomeric nucleosides and metal cation, we first characterized the structures of individual assemblies formed by G **1** and isoG **2** in the presence of Ba^{2+} picrate. Proton NMR showed that G **1** extracts Ba^{2+} picrate from water into CD_2Cl_2 to give a hydrogen-bonded complex with 8 equiv. of nucleoside bound to each Ba^{2+} (Fig. 1D). A crystal structure of [G **1**]$_{16}$·2[BaPic$_2$] indicated that 16 units of G **1** associate around two Ba^{2+} cations to form a G-quadruplex with four stacked G-quartets.[15b] Proton NMR experiments confirmed that this hexadecamer retains its structure in CD_2Cl_2 solution.[15c] NMR integration also showed that

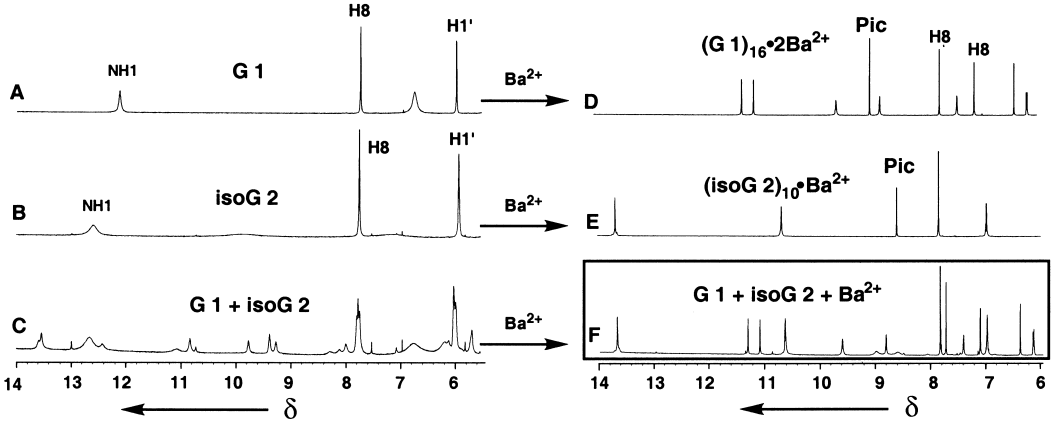

Figure 1. A series of ^{1}H NMR spectra in CD_2Cl_2 at rt showing the region from δ 14.0–6.0 ppm. (A) Recrystallized G **1** (11 mM); (B) recrystallized isoG **2** (11 mM); (C) an equimolar mixture of G **1** (5.5 mM) and isoG **2** (5.5 mM) 1 day after mixing; (D) recrystallized [G **1**]$_{16}$–2Ba^{2+} hexadecamer; (E) recrystallized [isoG **2**]$_{10}$–Ba^{2+} decamer; (F) an equimolar mixture of G **1**(5.5 mM) and isoG **2** (5.5 mM) after extraction of Ba^{2+}(Pic)$_2$ from water.

isoG **2** extracts Ba^{2+} picrate from water into CD_2Cl_2 to give a complex with a 5:1 nucleoside–picrate stoichiometry (Fig. 1E), consistent with a decamer, [isoG **2**]$_{10}$·[$BaPic_2$].

We next used an equimolar mixture of G **1** and isoG **2** to extract Ba^{2+} picrate from water into CD_2Cl_2 (Fig. 1F). After the extraction, only ^{1}H NMR signals for the two separate complexes, [G **1**]$_{16}$·2Ba^{2+} and [isoG **2**]$_{10}$·Ba^{2+}, were present. The spectrum in Fig. 1F is essentially a composite of spectra obtained from the individual nucleoside complexes (Fig. 1D and E). In Fig. 1F, there was no NMR evidence for cross-association of these two isomers in the presence of Ba^{2+} picrate.

These experiments demonstrate the cation's central role in expressing the hydrogen-bonding and base-stacking information embedded in the nucleoside monomers.[23] Both G **1** and isoG **2** self-associate essentially quantitatively upon addition of Ba^{2+} picrate. The two isomers, each with its own unique hydrogen bonding pattern, are completely sorted into structures composed of G-quartets and isoG pentamers, provided a Ba^{2+} cation is available to direct self-recognition.

4. The cation templates and stabilizes the self-assembled IsoG complex

In a second set of experiments, we used mass spectrometry to demonstrate the cation's crucial role in the self-assembly

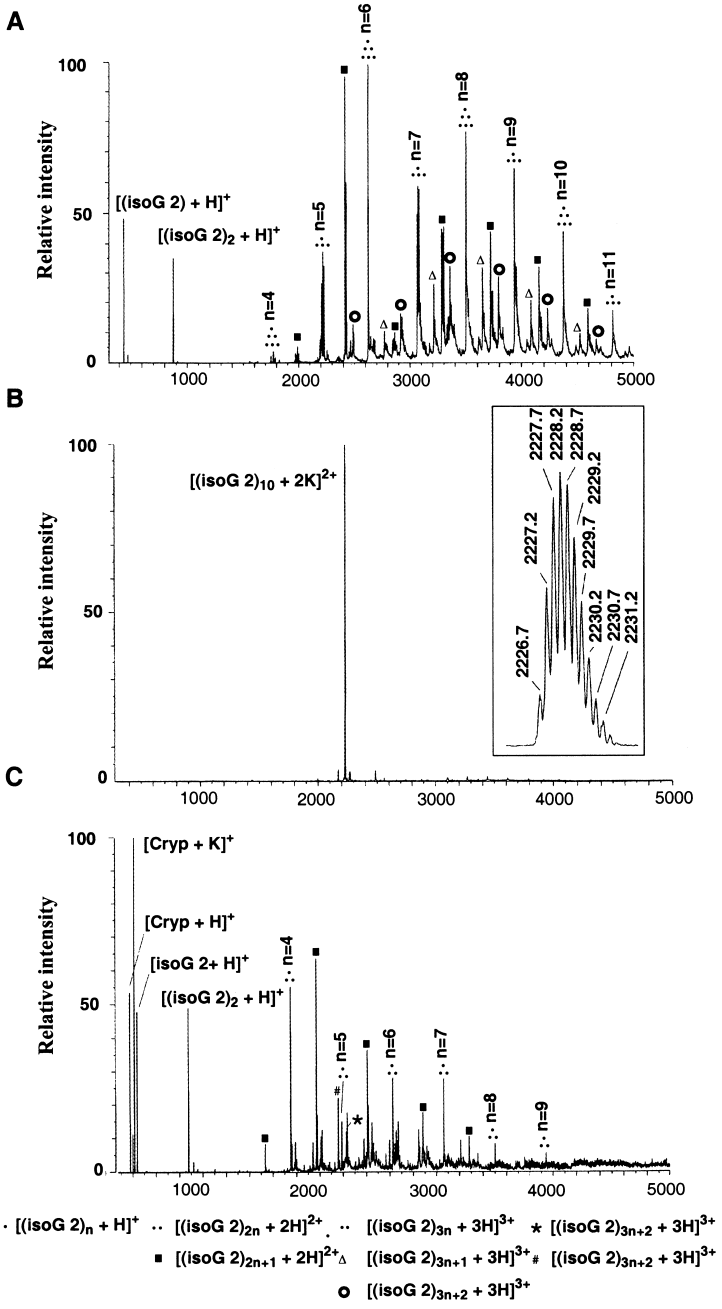

Figure 2. ESI mass spectra of (a) an acetone solution of isoG **2** (0.5 mM); (b) an acetone solution of isoG **2** (0.5 mM) and excess KI (0.5 mM) 15 min after mixing, the inset shows the experimental isotope pattern; (c) 15 min after addition of [2.2.2]-cryptand (0.5 mM) to the mixture from spectrum (b).

of isoG **2**. In addition to X-ray crystallography and NMR spectroscopy, electrospray ionization mass spectrometry (ESI-MS)[24,25] and matrix-assisted laser desorption[26] mass spectrometry have emerged as powerful techniques for the characterization of hydrogen-bonded complexes. To carry out ESI-MS from organic solvents the complex needs to be charged, often requiring an ion-labeling step.[25,26] Self-assembling ionophores from lipophilic nucleosides such as isoG **2** can be directly analyzed by ESI-MS since a cation is part of the complex.

Our ESI-MS experiments with isoG **2** clearly show that a cation is required to template and stabilize a defined aggregate. First, a 0.5 mM acetone solution of isoG **2** gave a series of peaks with charge states of one, two and three (Fig. 2A). Protons provide the charge needed for ESI-MS detection. The numerous high-molecular species, each differing by one isoG **2** unit, show isoG's propensity to form non-specific aggregates in low dielectric media.[27] With excess KI (0.5 mM) added to the solution of isoG **2** the ion pattern changed significantly; a new peak at 2228.2*m/z* dominated the spectrum (Fig. 2B). This peak corresponds to a species with a 5:1 ratio of isoG **2** and K^+. High-resolution measurements gave a 0.5 amu spacing in the isotopic distribution, indicating an ion with +2 charge and a formula of [isoG **2**]$_{10}$·[2K]$^{2+}$. This doubly charged isoG decamer may arise from two pentamers [isoG **2**]$_5$·[K]$^+$ associating during desolvation, or a second, lower-affinity K^+ cation may add to the [isoG **2**]$_{10}$·[K]$^+$ decamer. Importantly, addition of [2.2.2]-cryptand, a potent K^+ ionophore,[28] destroys the [isoG **2**]$_{10}$·[2K]$^{2+}$ assembly with regeneration of aggregates of variable stoichiometry (Fig. 2C).

These ESI-MS experiments demonstrate that cations are needed to convert a collection of non-specific aggregates into a single, stable species composed of [isoG **2**]$_5$ pentamer units. This ESI-MS experiment also illustrates how a template can shift the equilibrium of a dynamic combinatorial library.[23,29] A cyclic isoG pentamer is probably unstable without a cation to neutralize the charge density from the five oxygens that point into the cavity. Indeed, molecular dynamics calculations on DNA G-quartets concluded that removal of Na^+ cations from the G-quartet resulted in '…immediate (picosecond-scale) destabilization of the structure.'[30]

5. The hydrogen-bonded pentamer and cation exchange as a single unit

In non-covalent assemblies, individual building blocks and encapsulated guests can exchange with 'free' components in solution.[31,32] Studying these dynamic processes should provide a better understanding of the assembly and dissociation mechanisms, which in turn will guide design of new and improved self-assembling systems.

An X-ray crystal structure[16] showed that isoG **2** binds Cs^+ to form a sandwich decamer [isoG **2**]$_{10}$·[Cs]$^+$. We recently probed some dynamic properties of [isoG **2**]$_{10}$·[Cs]$^+$ in organic solvents.[5] Using ^{133}Cs NMR and ^{1}H–^{1}H EXSY NMR we found that the Cs^+ guest exchanges with free Cs^+ 40,000 times faster than the bound isoG **2** ligand exchanges with *free* isoG **2**. We also found that the decamer's kinetic stability depends on the M^+ guest, ligand exchange being much slower for the Cs^+ decamer as compared to the Li^+ decamer.

Formation of [isoG **2**]$_{10}$·[Cs]$^+$ is highly cooperative; the Cs^+ pentamer is never observed during ^{1}H and ^{133}Cs NMR titration experiments because it is immediately converted into the decamer.[5,16] The situation is different, however, for self-association of isoG **2** in the presence of the other alkali metal cations. With Li^+, Na^+, K^+ and Rb^+, isoG **2** can self-associate to give two hydrogen-bonded complexes: an open-faced pentamer and a sandwich decamer.[5] NMR titrations in $CDCl_3$ with isoG **2** and $M^+Ph_4B^-$ salts indicate that the pentamer is formed first, followed by the decamer (Scheme 5).[5] We set out to determine how isoG **2** and the cation exchange places between the pentamer and decamer complexes. Pentamer–decamer exchange may be a unimolecular, dissociative process or a bimolecular, associative process. In short, the isoG **2** ligand and the cation guest could dissociate from one complex as single pieces and then insert themselves into the other complex, or an intact [isoG **2**]$_5$·[M]$^+$ unit might migrate during pentamer–decamer exchange. As described next, dynamic multi-

Scheme 5. IsoG **2** binds cations in organic solvents to form [isoG **2**]$_5$·M^+ pentamer and [isoG **2**]$_{10}$·M^+ decamer complexes.

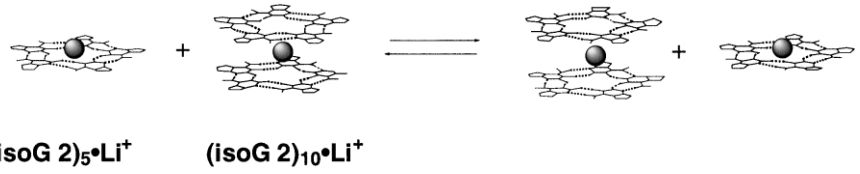

Scheme 6. Exchange of the Li^+ guest and isoG **2** host between (isoG **2**)$_5$·Li^+ and (isoG **2**)$_{10}$·Li^+ as an associative process, with (isoG **2**)$_5$·Li^+ exchanging as a single unit.

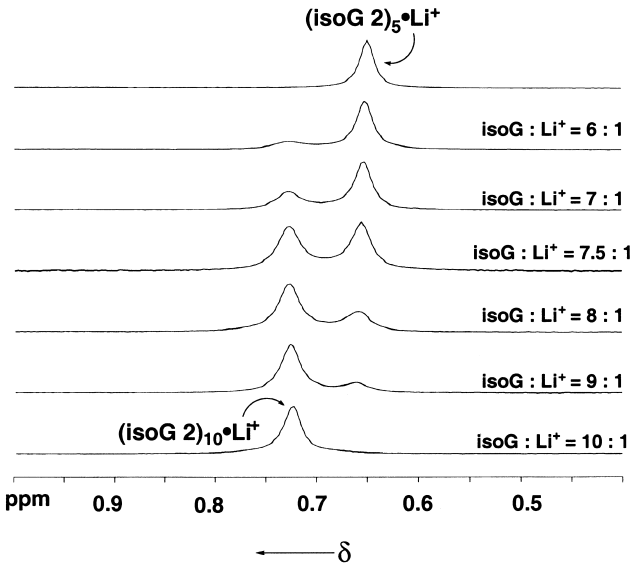

Figure 3. A series of ^{7}Li NMR spectra in $CDCl_3$ at rt. The top spectrum is of [isoG **2**]$_5$·$Li^+PH_4B^-$ prepared by the solid–liquid extraction of $LiPH_4B$ by isoG **2**. The other spectra were produced by titration of 'free' isoG **2** into the solution of [isoG **2**]$_5$·$Li^+PH_4B^-$.

nuclear NMR indicates that the latter process dominates (Scheme 6).

Lithium-7 is a relatively sensitive and abundant NMR active nucleus (I=3/2, 92.6% natural abundance) that can give reasonably sharp signals for coordination complexes with high-symmetry.[33] We reasoned that a ^{7}Li, ^{1}H NMR study of the [isoG **2**]$_n$·$[Li]^+$ complexes would be ideal for comparing ligand and cation exchange between a self-assembled isoG pentamer and decamer. Indeed, isoG **2** binds Li^+ to form both [isoG **2**]$_5$·$[Li]^+$ and [isoG **2**]$_{10}$·$[Li]^+$ and the two different complexes can be distinguished by ^{1}H and ^{7}Li NMR in $CDCl_3$ since both the Li^+ cation and the nucleoside undergo slow exchange on the NMR chemical shift timescale. By monitoring the ^{1}H NMR dynamics of the isoG **2** ligand and the ^{7}Li NMR dynamics of the Li^+ guest we have begun to probe the mechanistic details of pentamer–decamer exchange.

Depending on the conditions, the pentamer [isoG **2**]$_5$·$[Li]^+Ph_4B^-$, decamer [isoG **2**]$_{10}$·$[Li]^+Ph_4B^-$, or both, can be generated and observed in $CDCl_3$. Solid–liquid extraction of $LiPh_4B$ by isoG **2** gives quantitative formation of [isoG **2**]$_5$·$[Li]^+Ph_4B^-$, as determined by ^{1}H NMR integration of the signals corresponding to isoG **2** and the tetraphenylborate counterion. The [isoG **2**]$_5$·$[Li]^+$ pentamer obtained from the solid–liquid extraction has a single, relatively sharp ^{7}Li NMR peak at δ 0.65 ppm with a 4.6 Hz linewidth (Fig. 3A). Titration of isoG **2** ligand into the pentamer solution resulted in the appearance of a second, sharp ^{7}Li NMR peak at δ 0.74 ppm (Fig. 3B). When the isoG **2**/$LiPh_4B$ composition reached a 10:1 ratio, the pentamer's ^{7}Li NMR signal at δ 0.65 ppm had disappeared and only the decamer's ^{7}Li NMR signal at δ 0.74 ppm remained (Fig. 3). At isoG **2**/$LiPh_4B$ ratios between 5:1 and 10:1, both the pentamer's and decamer's ^{7}Li NMR signals could be separately observed in $CDCl_3$ at room temperature The ^{1}H NMR data was also consistent with the ^{7}Li NMR data. Upon addition of *free* isoG **2** to a solution of [isoG **2**]$_5$·$[Li]^+Ph_4B^-$ in $CDCl_3$, the pentamer's ^{1}H NMR peaks decreased, while a new set of peaks corresponding to [isoG **2**]$_{10}$·$[Li]^+Ph_4B^-$ appeared (Fig. 4). Both the Li^+-filled pentamer and decamer are kinetically stable species that can be monitored using multinuclear NMR spectroscopy.

We are concerned with how two different supramolecular complexes swap components. Since [isoG **2**]$_5$·$[Li]^+$ and [isoG **2**]$_{10}$·$[Li]^+$ gave separate ^{1}H and ^{7}Li NMR peaks in $CDCl_3$, we independently monitored pentamer–decamer exchange with two-dimensional ^{7}Li–^{7}Li and ^{1}H–^{1}H EXSY experiments on the same sample.[34,35] The NMR-derived pseudo-first-order rate constants for exchange (k_{app}), and thus the mean lifetimes (τ), for the hydrogen-bonded ligand (^{1}H–^{1}H EXSY) and the Li guest (^{7}Li–^{7}Li EXSY)[36] were both calculated from integration of EXSY diagonal cross peaks and off-diagonal cross peaks using

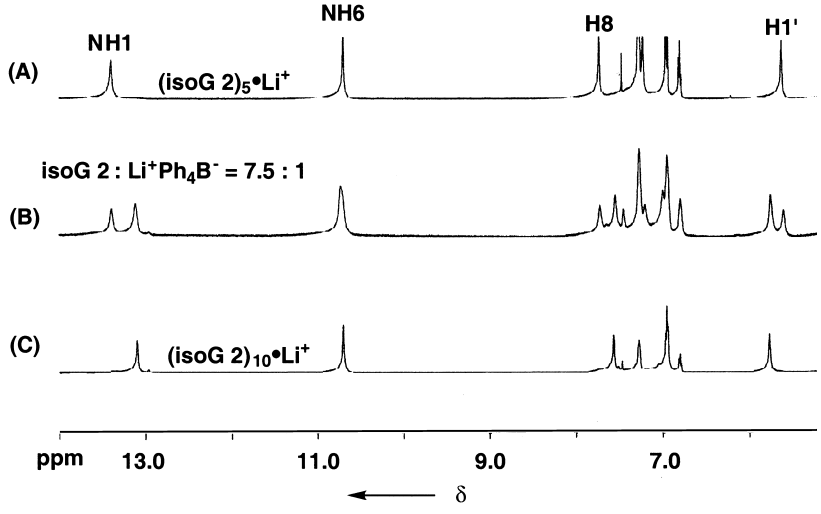

Figure 4. A series of ^{1}H NMR spectra in $CDCl_3$ at rt: (a) [isoG **2**]$_5$·$Li^+PH_4B^-$ prepared by the solid–liquid extraction of $LiPH_4B$ by isoG **2**; (b) a sample produced by addition of 2.5 equiv. of 'free' isoG **2** to [isoG **2**]$_5$·$Li^+PH_4B^-$; (c) [isoG **2**]$_{10}$·Li^+PH_4B; produced by addition of 5 equiv. of 'free' isoG **2** into the solution of [isoG **2**]$_5$·Li^+PH_4B.

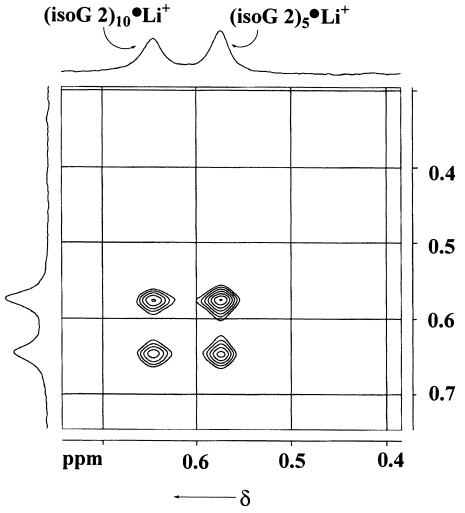

Figure 5. A contour plot from a ^{7}Li–^{7}Li EXSY experiment in $CDCl_3$ at rt. The sample contained a 1:1 molar ratio of [isoG **2**]$_5$·Li^+ and [isoG **2**]$_{10}$·Li^+ with a nominal isoG **2** concentration of 75 mM, [Li^+]=10 mM; τ_m=200 ms.

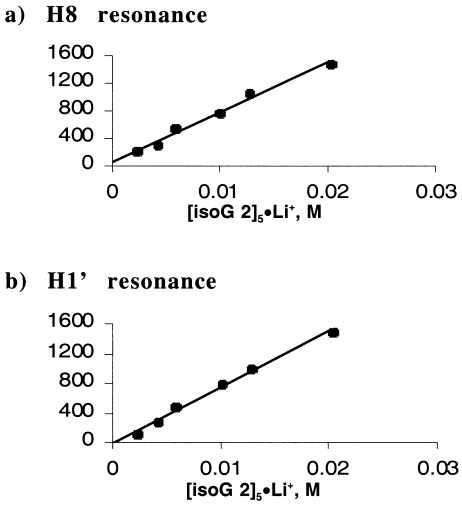

Figure 6. Pseudo-first order rate constant for pentamer–decamer exchange as a function of [isoG **2**]$_5$·Li^+ concentration in 50% $CDCl_3$–50% CD_3CN mixed solvent. Pseudo-first order rate constants were determined from line-shape analysis of (a) H8 and (b) H1′ resonances. Nominal concentrations of isoG **2** were varied from 22 to 189 mM with a constant 2:1 ratio of [isoG **2**]$_5$·Li^+/[isoG **2**]$_{10}$·Li^+. The slopes of the plots (7.4×10^4 $M^{-1}s^{-1}$) denote the second-order rate constant for pentamer–decamer exchange. The intercept's zero values are consistent with a bimolecular exchange mechanism.

Perrin's matrix method.[37] For a sample that contained 5 mM of [isoG **2**]$_5$·$[Li]^+$ and 2.5 mM of [isoG **2**]$_{10}$·$[Li]^+$ in $CDCl_3$ at room temperature, ^{7}Li–^{7}Li EXSY NMR (τ_m=100, 150 and 200 ms) revealed that the bound Li^+ guest has a mean lifetime of $\tau=0.26\pm0.04$ s (Fig. 5).[37] For the same sample, 2D ^{1}H–^{1}H EXSY NMR experiments showed that isoG **2** exchanges between the pentamer and decamer sites with a mean lifetime of $\tau=0.33\pm0.05$ s.[37] Since the Li^+ and isoG **2** exchange positions between pentamer and decamer at essentially the same rate, we suggest that ligand and cation exchange may correspond to the same process. In other words, an intact [isoG **2**]$_5$·$[Li]^+$ pentamer could be involved in the exchange without any significant dissociation of the cation-filled, hydrogen-bonded pentamer.

The EXSY experiments in $CDCl_3$ allowed us to evaluate dynamic processes at a single concentration in a solvent where exchange is slow on the chemical shift time-scale, but fast on the T_1 relaxation time-scale. We also carried out 1D ^{1}H NMR experiments on a 1:1 mixture of [isoG **2**]$_5$·$[Li]^+$ and [isoG **2**]$_{10}$·$[Li]^+$ in 50% CD_3CN–50% $CDCl_3$, a solvent where pentamer–decamer exchange is significantly faster on the NMR chemical shift time-scale. This approach enabled us to readily determine the exchange rate as a function of concentration, and thereby gain insight into the general exchange mechanism. If pentamer–decamer is an associative process then the exchange rate, and the ^{1}H NMR linewidth, should increase with increasing concentration of the isoG complexes. We used ^{1}H NMR line-shape analysis to calculate pseudo-first order rate constants for pentamer-decamer exchange in 50% CD_3CN–50% $CDCl_3$. Fig. 6 shows that a plot of [isoG **2**]$_5$ concentration vs rate constant is linear with a positive slope and a *y*-intercept that extrapolates to zero. The NMR pseudo-first order rate constant increases significantly with increasing concentration of [isoG **2**]$_5$·$[Li]^+$, and the plot's slope gives a second-order rate constant of $7.3–7.6\times10^4$ M^{-1} s^{-1}.

Taken together, our ^{7}Li and ^{1}H NMR data are consistent with the Li^+-filled pentamer migrating as a unit during a bimolecular exchange process. That [isoG **2**]$_5$·$[Li]^+$ remains intact during exchange, again underscores the structural stability of a cation-filled isoG pentamer. It is unlikely that an individual isoG **2** ligand first dissociates from one hydrogen-bonded complex before entering into the other hydrogen-bonded complex. Proton NMR data in the more polar solvent CD_3CN also argues strongly against such a dissociative mechanism. In that solvent, ligand exchange is fast between [isoG **2**]$_5$·$[Li]^+$ and [isoG **2**]$_{10}$·$[Li]^+$, as only a single set of ^{1}H NMR resonance are observed at room temperature for a 1:1 mixture of pentamer and decamer (1–10 mM concentration). In sharp contrast, ligand exchange is much slower between 'free' isoG **2** and [isoG **2**]$_{10}$·$[Li]^+$ in CD_3CN, as two sets of ^{1}H NMR signals are present at room temperature. An associative mechanism implies formation of a transition-state structure consisting of three hydrogen-bonded pentamers and two cations. We are carrying out other NMR and ESI-MS labeling experiments that may help distinguish between possible bimolecular mechanisms for pentamer–decamer exchange. We hope to report on these experiments soon.

6. Summary

These studies have furthered our understanding of how lipophilic nucleosides such as isoG **2** self-assemble. These compounds need a cation to form discrete, higher-ordered structures. The cation plays a central role in controlling the structure and dynamics of this self-assembled system. In many ways, this 'organic' model system mimics the structural complexity often found in biological systems. These self-assembled ionophores certainly have different levels of organization. For example, isoG **2** has self-complementary hydrogen bonding faces that are specifically utilized to form hydrogen-bonded macrocycles only upon cation coordination. This cation-induced self-assembly of

hydrogen-bonded macrocycles then progresses further to give stacked layers stabilized by base–base stacking and ion–dipole interactions. Thus, the cation 'seeds' formation of a complex but hierarchical supramolecular structure from a simple building block. As such, these lipophilic nucleosides should be excellent models for better understanding the structure and properties of natural systems such as the DNA G-quadruplexes.[17] Moreover, these self-assembling nucleosides should inspire the design of new building blocks for the construction of nano- and micron-sized assemblies.[11,38]

The design, characterization and development of self-assembled systems have a number of challenges. First, one must establish the system's structure. Modern analytical tools, including X-ray crystallography, NMR spectroscopy, and mass spectrometry have enabled the structure determination of some impressive supramolecular systems.[1–4] Next, there is function. Are the supramolecular complexes useful? Do they bind and transport guests or catalyze reactions? A firm understanding of mechanism is essential for better control of structure and function. How do the systems assemble and dissociate? How are the supramolecular properties influenced by changes in individual components? Are there kinetically stable intermediates along the path from the monomeric building blocks to the thermodynamic assembly? Unraveling the mechanisms of self-assembly processes is one of the field's foremost challenges,[31,32] and the study of lipophilic nucleosides such as G **1** and isoG **2** provides an excellent model for gaining a better understanding of self-assembly.

7. Experimental

7.1. General

Guanosine **1**, isoG **2** and potassium picrate were prepared following published methods.[15,16] *Warning*. Picric acid and picrate salts should be handled and stored with the appropriate precautions. Both nucleoside derivatives G **1** and isoG **2** were recrystallized from isopropanol prior to use. The [2.2.2]-cryptate and $LiPh_4B$ [$3(CH_2OCH_3)_2$] were purchased from Aldrich. Other reagents and solvents were obtained from commercial sources and used after standard purification. Deuterated NMR solvents were purchased from Cambridge Isotope Labs. The NMR data were collected on a Bruker DRX-500 or DRX-400 spectrometer. The 1D ^{1}H NMR spectra were obtained with a 10 s delay to ensure accurate integration. The probe temperature was controlled to +0.1°C.

7.1.1. In situ formation of (G 1)$_{16}$·2Ba^{2+}Pic$_4$ by liquid–liquid extraction. A solution of G **1** (5.0 mg, 11 μmol) in 1 mL of CD_2Cl_2 was stirred with an aqueous solution of $BaCl_2$ and K^+ picrate (1 mL, 6 mM) at rt for 5 h. The organic layer was separated and centrifuged to remove residual water. A ^{1}H NMR spectrum for this complex was identical to that for crystalline (G **1**)$_{16}$·2Ba^{2+}Pic$_4$.[15c] In the ^{1}H NMR assignments below the subscripts a and b refer to the two sets of signals observed for the [G **1**]$_8$ octamer unit. (400 MHz, CD_2Cl_2): δ 11.31 (s, 1H, $NH1_a$), 11.09 (s, 1H, $NH1_b$), 9.61 (s, 1H, N2 H_a), 9.00 (s, 1H, Pic), 8.82 (s, 1H, N2 H_b), 7.74 (s, 1H, $H8_a$), 7.42 (s, 1H, N2 H_b), 7.11 (s, 1H, $H8_b$), 6.38 (s, 1H, $H1'_a$), 6.14 (d, 1H, $H2'_a$, J=6.0 Hz), 5.89 (s, 1H, N2 H_a), 5.70 (d, 1H, $H2'_b$, J=4.4 Hz), 5.59 (d, 1H, $H1'_b$, J=3.4 Hz), 4.79 (d, 1H, $H3'_a$, J=6.0 Hz), 4.25–4.17 (m, 4H, H4′, H5′), 4.09 (d, 1H, $H3'_b$, J=6.4 Hz), 3.23–3.19 (m, 2H, H5′), 1.59 (s, 3H, CH_{3a}), 1.56 (s, 3H, CH_{3b}), 1.53 (s, 3H, CH_{3a}), 1.48 (s, 3H, CH_{3b}), 0.88 (s, 9H, Si–tBu$_a$), 0.53 (s, 9H, Si–tBu$_b$), 0.17 (s, 6H, Si–CH_{3a}), −0.36 (s, 6H, Si–CH_{3b}).

7.1.2. In situ formation of (isoG 2)$_{10}$·Ba^{2+}Pic$_2$ by liquid–liquid extraction. A solution of isoG **2** (5.0 mg, 11 μmol) in 1 mL of CD_2Cl_2 was stirred with an aqueous solution of $BaCl_2$ and K^+ picrate (1 mL, 6 mM) at rt for 5 h. The organic layer was separated and washed by distilled water (3×5 mL). The yellow organic layer was separated for NMR analysis. ^{1}H NMR (400 MHz, CD_2Cl_2): δ 13.68 (s, 1H, NH1), 10.67 (s, 1H, N6 H_A), 8.58 (s, 0.4H, Pic), 7.82 (s, 1H, H8), 6.96 (s, 1H, N6 H_B), 5.47 (s, 1H, H1′), 4.86 (m, 2H, H2′and H3′), 4.46 (s, 1H, H4′), 3.98–3.79 (m, 2H, H5′), 2.12 (s, 3H, CH_3), 1.41 (s, 3H, CH_3), 0.85 (s, 9H, Si–tBu), 0.08 (s, 3H, Si–CH_3), 0.07 (s, 3H, Si–CH_3).

7.1.3. Self-sorting experiment with G 1 and isoG 2. A solution of G **1** (5.0 mg, 11 μmol) and isoG **2** (5.0 mg, 11 μmol) in 2 mL of CD_2Cl_2 was stirred with an aqueous solution of $BaCl_2$ and K^+ picrate (1 mL, 10 mM) at rt for 5 h. The organic layer was separated, washed with distilled water (3×5 mL) and analyzed by ^{1}H NMR.

7.2. Electrospray ionization mass spectra

ESI-MS were collected using the first mass spectrometer of a JEOL Ltd (Tokyo, Japan) HX110/HX110 four sector mass spectrometer equipped with an Analytica of Brandford Inc. (Brandford, CT) thermally assisted electrospray ion source. Solutions were infused into the source at 1 μL/min using a syringe pump and the interfacing capillary was heated at 90°C. Resolution was set to 1000 or higher, with a mass accuracy of 0.03% or better. A scan time of 90 s was used for the m/z range of 0–6000. Each spectrum represents the averaged profile of 10 scans recorded by the JEOL MP7000 data system.

Portions of recrystallized isoG **2** were dissolved in anhydrous HPLC-grade acetone (J. T. Baker) to give solutions with nominal isoG **2** concentration of 0.5 mM. Solutions of KI in acetone were added to the isoG **2** solution so that the KI concentration was 0.5 mM. These solutions were allowed to equilibrate at rt for 15 min prior to ESI-MS analysis.

7.3. 1D ^{7}Li nuclear magnetic resonance

The ^{7}Li NMR spectra were obtained on a Bruker DRX-500 NMR spectrometer operating at 194.4 MHz. The ^{7}Li NMR spectra were referenced to an external standard of 3.0 M LiCl in D_2O (0 ppm at 298 K). The spectral width was 1800 Hz. The 90° pulse time was 11 μs. Inversion-recovery measurements showed that the T_1 values were 390 ms for [isoG **2**]$_5$·$[Li]^+$ and 300 ms for [isoG **2**]$_{10}$·$[Li]^+$. A relaxation delay was set to 1 s.

7.3.1. Formation of the Li^+ pentamer (isoG 2)$_5$–$LiPh_4B$. A solution of isoG **2** (4.4 mg, 0.010 mMol) in 1.0 mL of $CDCl_3$ was stirred over 15.0 mg of solid $LiPh_4B\cdot[3(CH_2OCH_3)_2]$ for 12 h at rt. The suspension was filtered, and the solution was washed with distilled water (2×1 mL) and then characterized by ^1H and ^7Li NMR. The ^1H NMR (500 MHz, $CDCl_3$): δ 13.39 (s, 1H, NH1), 10.69 (s, 1H, N6 H_A), 7.72 (s, 1H, H8), 7.22 (m, 1.6H, BPh_4^- *ortho*-), 7.22 (m, 1.6 H, BPh_4^- *meta*-), 6.79 (m, 0.8H, BPh_4^- *para*-), 6.77 (s, 1H, N6 H_B), 5.62 (s, 1H, H1′), 4.82 (m, 2H, H2′ and H3′), 4.48 (s, 1H, H4′), 3.93–3.76 (m, 2H, H5′,H5″), 1.75 (s, 3H, CH_3), 1.36 (s, 3H, CH_3), 0.79 (s, 9H, Si–*t*Bu), −0.01 (s, 3H, Si–CH_3), −0.02 (s, 3H, Si–CH_3). ^7Li NMR (194 MHz, $CDCl_3$): δ 0.65 (s).

7.3.2. Formation of (isoG 2)$_{10}$–$LiPh_4B$. To the $CDCl_3$ solution of (isoG **2**)$_5$–$LiPh_4B$ pentamer, addition of 5 equiv. of isoG **2** ligand gave formation (isoG **2**)$_{10}$–$LiPh_4B$ decamer. ^1H NMR (500 MHz, $CDCl_3$): δ 13.10 (s, 1H, NH1), 10.70 (s, 1H, N6 H_A), 7.56 (s, 1H, H8), 7.27 (m, 0.8 H, BPh_4^- *ortho*-), 6.95 (m, 0.8 H, BPh_4^- *meta*-); 6.83 (m, 0.4 H, BPh_4^- *para*-), 6.92 (s, 1H, N6 H_B), 5.77 (s, 1H, H1′), 4.96 (s, 1H, H1′), 4.78 (s, 1H, H3′), 4.49 (s, 1H, H4′), 3.88–3.74 (m, 2H, H5′,H5″), 1.77 (s, 3H, CH_3), 1.37 (s, 3H, CH_3), 0.80 (s, 9H, Si–*t*Bu), −0.01 (s, 3H, Si–CH_3), −0.02 (s, 3H, Si–CH_3) ^7Li NMR (194 MHz, $CDCl_3$): δ 0.74 (s).

7.4. 2D ^1H–^1H EXSY measurements

Samples for the 2D EXSY NMR experiments were prepared by adding 2.5 equiv. of 'metal-free' isoG **2** to a solution of [isoG **2**]$_5\cdot Li^+$ in $CDCl_3$. The resulting mixture of [isoG **2**]$_5\cdot Li^+$ and [isoG **2**]$_{10}\cdot Li^+$ was characterized by ^1H and ^7Li NMR. The 2D EXSY NMR experiments were recorded using the standard NOESY (Bruker XWINNMR Version 2.0) pulse sequence (90°–t_1–90°–t–90°–acq.). Experiments were performed at 25°C, with mixing times varied between 100 and 500 ms. The experiments were conducted in the phase-sensitive mode using the TPPI method. A relaxation delay was set at 4.0 s. The spectral width was 8003 Hz in each dimension. A total of 32 scans were collected for each time increment. A total of 512 serial files were collected, resulting in a data matrix of 512×2048. A line broadening of 2 Hz in the F2 dimension and 7 Hz in the F1 dimension was imposed prior to Fourier transformation. Sizable off-diagonal peaks were observed, indicating exchange of isoG **2** between pentamer [isoG **2**]$_5\cdot Li^+$ and decamer [isoG **2**]$_{10}\cdot Li^+$. The crosspeak volume intensity, I_{ij} (i, j=pentamer, decamer) was measured using the WinNMR program (Bruker). The relationship between the 2D peak intensities (I_{ij}) at some specified mixing time (τ_m) and the exchange rate constants is given by following equation

$$I_{ij}(\tau_m) = (e^{-R\tau m})_{ij} M_j^\circ$$

where M°_j is the equilibrium magnetization of the nuclei in site j and R has off-diagonal elements $R_{ij}=-k_{ji}$, where k_{ji} is the first-order rate constant for chemical exchange from site j to site i. The rate constants k_{ij} and k_{ji} were calculated using Perrin's matrix method.[37] Calculations were done using MathCAD 7 software (MathSoft Inc.). The mean lifetime of exchange τ was calculated from the relationship to the measured first-order rate constants k_{ij} and k_{ji}, $\tau=1/k$ (k is the average exchange rate constant, $k=(k_{ij}+k_{ji})/2$).

7.5. ^7Li–^7Li EXSY

The 2D ^7Li–^7Li NOESY experiments were recorded at 25°C with mixing times of 100, 150 and 200 ms using the standard NOESY (Bruker XWINNMR Version 2.0) pulse sequence (90°–t_1–90°–t–90°–acq). The experiments were conducted in the phase-sensitive mode using the TPPI method. The data were collected with a relaxation delay of 1.0 s. The spectral width was 2914 Hz in each dimension. A total of 32 scans were collected for each time increment. A total of 512 serial files were collected, resulting in a data matrix of 512×2048. Data processing and EXSY rate analysis was carried out as described above for the ^1H–^1H EXSY data.

7.6. Pentamer–decamer exchange in 50% CD_3CN–50% $CDCl_3$

Samples were prepared to evaluate [isoG **2**]$_5\cdot Li^+$–[isoG **2**]$_{10}\cdot Li^+$ exchange. In the binary solvent of 50% CD_3CN–50% $CDCl_3$, a 188.3 mM solution of isoG **2** and 29 mM solution of $LiBPh_4\cdot 3(CH_3OC_2H_4OCH_3)$ was prepared by dissolving 56.2 mg of isoG **2** and 11.8 mg of $LiBPh_4\cdot 3(CH_3OC_2H_4OCH_3)$ in 0.792 g of solvent. The actual density of binary solvent was determined as 1.162 g cm^{-3}. Thus, the ratio of isoG **2**/Li^+ was set to approximately 1:0.15, providing 2:1 [isoG **2**]$_5\cdot Li^+$/[isoG **2**]$_{10}\cdot Li^+$ ratio. Other samples were prepared from this stock solution by diluting with 50% $CDCl_3$–50% CD_3CN. Concentrations of isoG **2** and [isoG **2**]$_5\cdot Li^+$ were varied from 188 to 22 mM and from 20 to 2.3 mM, respectively.

The apparent pseudo-first order rate constants for [isoG **2**]$_5\cdot Li^+$–[isoG **2**]$_{10}\cdot Li^+$ exchange were assessed from the line-shape analysis of H8 and H1′ resonances according to the equation

$$k = \pi\Delta\nu_0^2/(\nu_{1/2} - \nu_{01/2})$$

where k is a pseudo-first order rate constant, $\Delta\nu_0$ is a difference of resonances in exchange (Hz), $\nu_{1/2}$ is width of peak (Hz) of interest at the half-height, $\nu_{01/2}$ is width of the same peak under conditions of no exchange. The $\Delta\nu_0$ and $\nu_{01/2}$ values were determined from independent NMR measurements of [isoG **2**]$_5\cdot Li^+$ and [isoG **2**] $_{10}\cdot Li^+$.

Acknowledgements

This research was sponsored by the Separations and Analysis Program, Division of Chemical Sciences, Office of Basic Energy Sciences, U.S. Department of Energy. J. D. thanks the Dreyfus Foundation for a Teacher-Scholar Award. We thank Professor Giovanni Gottarelli for helpful comments during the manuscript's preparation.

References

1. For reviews on self-assembly: (a) Lawrence, D. S.; Jiang, T.; Levett, M. *Chem. Rev.* **1995**, *95*, 2229–2260. (b) Philp, D.;

Stoddart, J. F. *Angew. Chem., Int. Ed. Engl.* **1996**, *35*, 1155–1196.
2. For reviews on self-assembly via hydrogen bonding: (a) Conn, M. M.; Rebek, Jr., J. *Chem. Rev.* **1997**, *97*, 1647–1668. (b) Krische, M. J.; Lehn, J.-M. *Struct. Bonding* **2000**, *96*, 3–29. (c) Zimmerman, S. C.; Corbin, P. S. *Struct. Bonding* **2000**, *96*, 63–94.
3. For reviews on self-assembly via coordination bonds: (a) Leininger, S.; Olenyuk, B.; Stang, P. J. *Chem. Rev.* **2000**, *100*, 853–907. (b) Swiegers, G. F.; Malefetse, T. J. *Chem. Rev.* **2000**, *100*, 3483–3537. (c) Fujita, M. *Struct. Bonding* **2000**, *96*, 177–201.
4. For a review on metal-templated self-assembly of hydrogen bonded systems: Linton, B.; Hamilton, A. D. *Chem. Rev.* **1997**, *97*, 1669–1680.
5. Cai, M.; Sidorov, V.; Lam, Y. F.; Flowers, R. A.; Davis, J. T. *Org. Lett.* **2000**, *2*, 1665–1668.
6. (a) Davis, J. T.; Tirumala, S.; Jenssen, J. R.; Radler, E.; Fabris, D. *J. Org. Chem.* **1995**, *60*, 4167–4176. (b) Davis, J. T.; Tirumala, S.; Marlow, A. L. *J. Am. Chem. Soc.* **1997**, *119*, 5271–5272.
7. (a) Gottarelli, G.; Masiero, S.; Spada, G. P. *Chem. Commun.* **1995**, 2555–2557. (b) Andrisano, V.; Gottarelli, G.; Masiero, S.; Heijne, E. H.; Pieraccini, S.; Spada, G. P. *Angew. Chem., Int. Ed.* **1999**, *38*, 2386–2388. (c) Masiero, S.; Gottarelli, G.; Pieraccini, S. *Chem. Commun.* **2000**, 1995–1996.
8. (a) Marlow, A. L.; Mezzina, E.; Spada, G. P.; Masiero, S.; Davis, J. T.; Gottarelli, G. *J. Org. Chem.* **1999**, *64*, 5116–5123. (b) Mezzina, E.; Mariani, P.; Itri, R.; Masiero, S.; Pieraccini, S.; Spada, G. P.; Spinozzi, F.; Davis, J. T.; Gottarelli, G. *Chem. Eur. J.* **2001**, *7*, 388–395.
9. (a) Lee, S. C.; Lamb, J. D.; Cai, M.; Davis, J. T. *J. Incl. Phenom.* **2001**, *40*, 51–57. For another promising approach towards building self-assembled ionophores using coordination bonds instead of hydrogen bonding, see: (b) Piotrowski, H.; Hilt, G.; Sculz, A.; Mayer, P.; Polborn, K.; Severin, K. *Chem. Eur. J.* **2001**, *7*, 3197–3208.
10. Marlow, A. L.; Davis, J. T. *Tetrahedron Lett.* **1999**, *40*, 3539–3542.
11. Sidorov, V.; Kotch, F. W.; El-Kouedi, M.; Davis, J. T. *Chem. Commun.* **2000**, 2369–2370.
12. (a) Harriman, A.; Kubo, Y.; Sessler, J. L. *J. Am. Chem. Soc.* **1992**, *114*, 388–390. (b) Nowick, J. S.; Chen, J. S.; Noronha, G. *J. Am. Chem. Soc.* **1993**, *115*, 7636–7644. (c) Schall, O. F.; Gokel, G. W. *J. Am. Chem. Soc.* **1994**, *116*, 6089–6100. (d) Sessler, J. L.; Wang, B.; Harriman, A. *J. Am. Chem. Soc.* **1995**, *117*, 704–714. (e) Zimmerman, S. C.; Schmitt, P. *J. Am. Chem. Soc.* **1995**, *117*, 10769–10770. (f) Sessler, J. L.; Wang, R. *Angew. Chem., Int. Ed.* **1998**, *37*, 1726–1729. (g) Gottarelli, G.; Masiero, S.; Mezzina, E.; Pieraccini, S.; Rabe, J. P.; Samori, P.; Spada, G. P. *Chem. Eur. J.* **2000**, *6*, 3242–3248.
13. For an isoG–G WC base pair: Groebke, K.; Hunziker, J.; Fraser, W.; Peng, L.; Diederichsen, U.; Zimmermann, K.; Holzner, A.; Leumann, C.; Eschenmoser, A. *Helv. Chim. Acta* **1998**, *81*, 375–474.
14. Forman, S. L.; Fettinger, J. C.; Pieraccini, S.; Gottarelli, G.; Davis, J. T. *J. Am. Chem. Soc.* **2000**, *122*, 4060–4067.
15. (a) Kotch, F. W.; Fettinger, J. C.; Davis, J. T. *Org. Lett.* **2000**, *2*, 3277–3280. (b) Shi, X. D.; Fettinger, J. C.; Davis, J. T. *Angew. Chem., Int. Ed.* **2001**, *40*, 2827–2831. (c) Shi, X. D.; Fettinger, J. C.; Davis, J. T. *J. Am. Chem. Soc.* **2001**, *123*, 6738–6739.
16. (a) Cai, M.; Marlow, A. L.; Fettinger, J. C.; Fabris, D.; Haverlock, T. J.; Moyer, B. A.; Davis, J. T. *Angew. Chem., Int. Ed.* **2000**, *39*, 1283–1285. (b) Shi, X.; Fettinger, J. C.; Cai, M. M.; Davis, J. T. *Angew. Chem., Int. Ed.* **2000**, *39*, 3124–3127.
17. Guschlbauer, W.; Chantot, J. F.; Thiele, D. J. *Biomol. Struct. Dynam.* **1990**, *8*, 491–511.
18. Gilbert, D. E.; Feigon, J. *Curr. Opin. Struct. Biol.* **1999**, *9*, 305–314.
19. Chaput, J. C.; Switzer, C. *Proc. Natl Acad. Sci. USA* **1999**, *96*, 10614–10619. For another report on Cs^+ binding by isoG-rich oligonucleotides, see: Seela, F.; Wei, C.; Melenewski, A.; Feiling, E. *Nucleosides, Nucleotides* **1998**, *17*, 2045–2052.
20. Sessler has shown that a conformationally constrained G nucleoside can form a G-quartet without a cation: Sessler, J. L.; Sathiosatham, M.; Doerr, K.; Lynch, V.; Abboud, K. A. *Angew. Chem., Int. Ed.* **2000**, *39*, 1300–1303.
21. (a) Rowan, S. J.; Reynolds, D. J.; Sanders, J. K. M. *J. Org. Chem.* **1999**, *64*, 5804–5814. (b) Taylor, P. N.; Anderson, H. L. *J. Am. Chem. Soc.* **1999**, *121*, 11538–11545.
22. Based on the relative broadness of ^{1}H NMR signals, self-sorting of G 1 and isoG 2 is not as efficient with K^+ as it is with Ba^{2+}. For recent studies on how divalent cations stabilize these lipophilic assemblies, see Ref. 15.
23. For reviews on dynamic combinatorial libraries: (a) Lehn, J.-M. *Chem. Eur. J.* **1999**, *5*, 2455–2463. (b) Cousins, G. R. L.; Poulsen, S. A.; Sanders, J. K. M. *Curr. Opin. Chem. Biol.* **2000**, *4*, 270–279.
24. For a review on the use of ESI-MS in supramolecular chemistry: Schalley, C. A. *Int. J. Mass Spectrom.* **2000**, *134*, 11–39.
25. For the use of ESI-MS to characterize hydrogen-bonded assemblies: (a) Russell, K. C.; Leize, E.; van Dorsselaer, A. *Angew. Chem., Int. Ed.* **1995**, *34*, 209–213. (b) Cheng, X.; Gao, Q.; Smith, R. D.; Simanek, E. E.; Mammen, E.; Whitesides, G. M. *J. Org. Chem.* **1996**, *61*, 2204–2206. (c) Schalley, C. A.; Castellano, R. K.; Brody, M. S.; Rudkevich, D. M.; Siuzdak, G.; Rebek, J. *J. Am. Chem. Soc.* **1999**, *121*, 4568–4579. (d) Schalley, C. A.; Martin, T.; Obst, U.; Rebek, J. *J. Am. Chem. Soc.* **1999**, *121*, 2133–2138. (e) Schalley, C. A.; Rivera, J. M.; Martin, T.; Santamaria, J.; Siuzdak, G.; Rebek, J. *Eur. J. Org. Chem.* **1999**, 1131–1325.
26. (a) Jolliffe, K. A.; Calama, M. C.; Fokkens, R.; Nibbering, N. M. M.; Timmerman, P.; Reinhoudt, D. N. *Angew. Chem., Int. Ed.* **1998**, *37*, 1247–1251. (b) Timmerman, P.; Jolliffe, K. A.; Calama, M. C.; Weidmann, J.-L.; Prins, L. J.; Cardullo, F.; Snellink-Ruel, B. H. M.; Fokkens, R. H.; Nibbering, N. M. M.; Shinkai, S.; Reinhoudt, D. N. *Chem. Eur. J.* **2000**, *6*, 4104–4115.
27. Concentration dependent changes in ^{1}H NMR chemical shifts, as well as ITC and VPO data, indicate that isoG **2** aggregates in organic solvents in the absence of a cation, see Ref. 5. An X-ray crystal structure also shows that, in the absence of templating cations, isoG **2** forms a one-dimensional ribbon held together by a chain of hydrogen bonds: Bryan, J. C., Davis, J. T., unpublished results. For a similar ribbon structure formed by lipophilic G derivatives in the absence of templating cations, see: Gottarelli, G.; Masiero, S.; Mezzina, E.; Spada, G. P.; Mariani, P.; Recanatini, M. *Helv. Chim. Acta* **1998**, *81*, 2078–2092.
28. Lehn, J.-M.; J, P.; Sauvage, J. P. *J. Am. Chem. Soc.* **1975**, *97*, 6700–6707.

29. Cousins, G. R. L.; Furlan, R. L. E.; Ng, Y.-F.; Redman, J. E.; Sanders, J. K. M. *Angew. Chem., Int. Ed.* **2001**, *40*, 423–428.
30. Spackova, N.; Berger, I.; Sponer, J. *J. Am. Chem. Soc.* **1999**, *121*, 5519–5534.
31. For a review on dynamic exchange in self-assembly: Rebek, Jr., J. *Acc. Chem. Res.* **1999**, *32*, 278–286.
32. (a) Mogck, O.; Pons, M.; Böhmer, V.; Vogt, W. *J. Am. Chem. Soc.* **1997**, *119*, 5706–5710. (b) Chapman, R. G.; Sherman, J. C. *J. Am. Chem. Soc.* **1998**, *120*, 9818–9826. (c) Folmer, B. J. B.; Sijbesma, R. P.; Kooijman, H.; Spek, A. L.; Meijer, E. W. *J. Am. Chem. Soc.* **1999**, *121*, 9001–9007. (d) Vysotsky, M. O.; Thondorf, I.; Böhmer, V. *Angew. Chem., Int. Ed.* **2000**, *39*, 1264–1267. (e) Hof, F.; Nuckolls, C.; Craig, S. L.; Martin, T.; Rebek, Jr., J. *J. Am. Chem. Soc.* **2000**, *122*, 10991–10996.
33. For application of ^{7}Li NMR, see: (a) Cahen, Y. M.; Dye, J. L.; Popov, A. I. *J. Phys. Chem.* **1975**, *79*, 1292–1295. (b) Cahen, Y. M.; Dye, J. L.; Popov, A. I. *J. Phys. Chem.* **1975**, *79*, 1289–1291. (c) Shamsipur, M.; Popov, A. I. *J. Phys. Chem.* **1986**, *90*, 5997–5999. (d) Brière, K. M.; Detellier, C. *J. Phys. Chem.* **1992**, *96*, 2185–2189. (e) Reich, H. J.; Borst, J. P.; Dykstra, R. R.; Green, D. P. *J. Am. Chem. Soc.* **1993**, *115*, 8728–8741. (f) Carlier, P. R.; Lo, C. W. S. *J. Am. Chem. Soc.* **1993**, *122*, 12819–12823.
34. Jeener, J.; Meier, B. H.; Bachmann, P.; Ernst, R. R. *J. Chem. Phys.* **1979**, *71*, 4546–4553.
35. For a review on EXSY NMR: Perrin, C. L.; Dwyer, T. *J. Chem. Rev.* **1990**, *90*, 935–967.
36. ^{7}Li–^{7}Li EXSY NMR: Brière, K. M.; Dettman, H. D.; Detellier, C. *J. Magn. Reson.* **1991**, *94*, 600–604.
37. Perrin, C. L.; Gipe, R. K. *J. Am. Chem. Soc.* **1984**, *106*, 4691–4696.
38. Fenniri, H.; Mathivanan, P.; Vidale, K. L.; Sherman, D. M.; Hallenja, K.; Wood, K. V.; Stowell, J. G. *J. Am. Chem. Soc.* **2001**, *123*, 3854–3855.